

**Morphologies-Controlled Synthesis of TiO₂/MoS₂ Nanocomposites for Enhanced
Visible-light Photocatalytic Activities**

Yuanqing Sun,^{a,c} Huihui Lin,^b Chuanxi Wang,^{*a} Qian Wu,^b Xiaojie Wang,^b and
Minghui Yang^{*a}

^a*Institute of New Energy Technology, Ningbo Institute of Industrial Technology,
Chinese Academy of Sciences, Ningbo, 315201, P. R. China*

E-mail addresses: wangcx@nimte.ac.cn; myang@nimte.ac.cn

^b*School of Chemical & Material Engineering, Jiangnan University, Wuxi 214122, P.
R. China.*

^c*State Key Laboratory of Heavy Oil Processing, College of Science, China University
of Petroleum, Beijing, 102249, P. R. China*

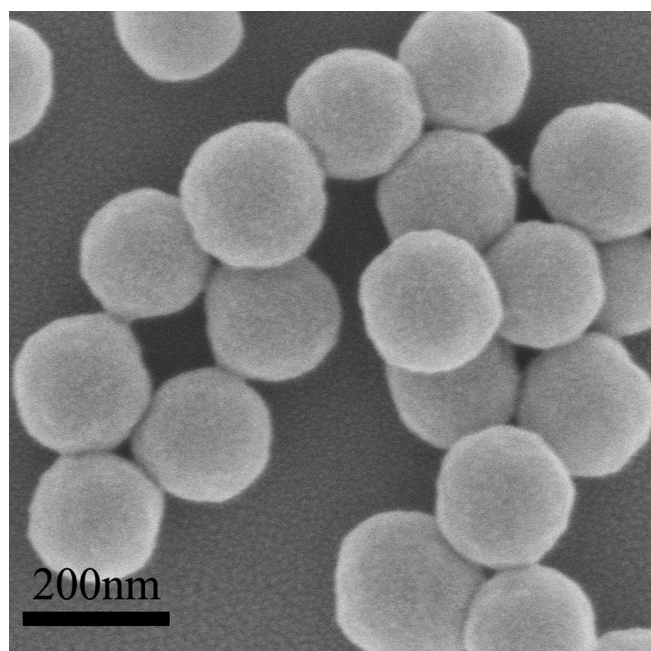


Figure S1 SEM image of TiO₂ microspheres.

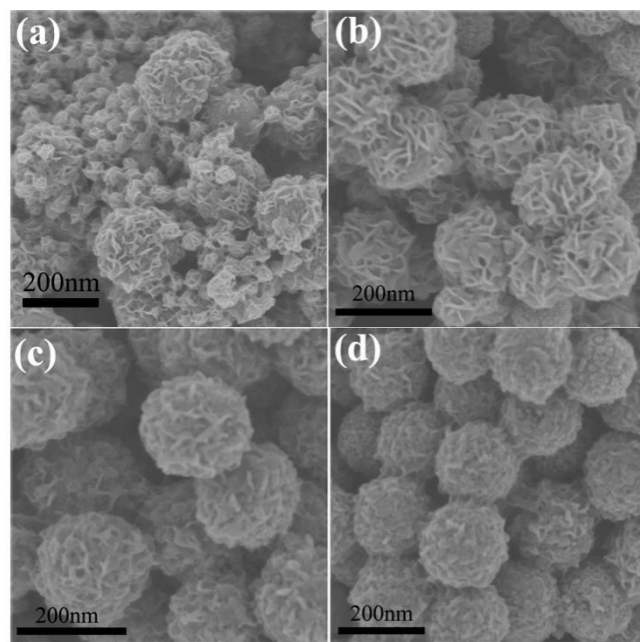


Figure S2 SEM images with different thickness of MoS₂ prepared by using various amounts of TiO₂ microspheres as seeds: (a) 1 mg·mL⁻¹; (b) 2 mg·mL⁻¹; (c) 3 mg·mL⁻¹; (d) 5 mg·mL⁻¹.

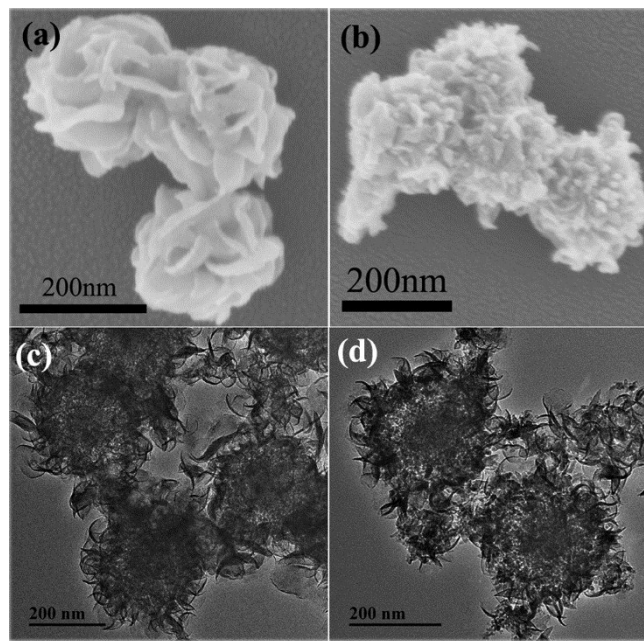


Figure S3. SEM (a, b) and TEM (c, d) images of MoS₂/TiO₂ yolk–shell structure synthesized by targeted etching for 0.5 h (a, c), 2 h (b, d), respectively.

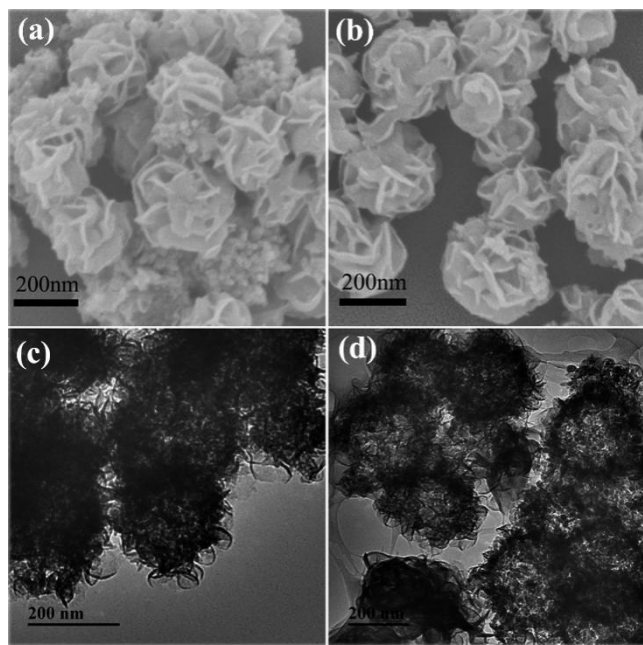


Figure S4. SEM (a, b) and TEM (c, d) images of MoS₂/TiO₂ hollow structure synthesized by targeted etching for 1 h (a, c), 3 h (b, d), respectively.

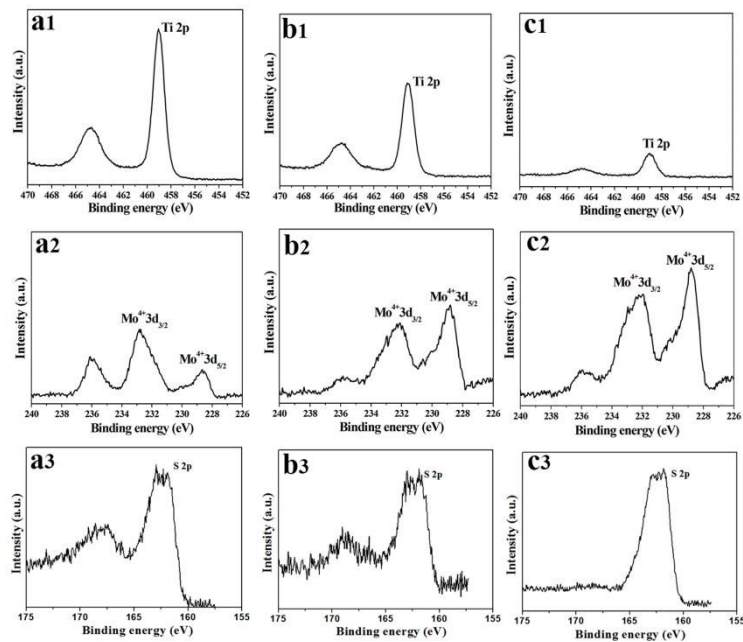


Figure S5 XPS spectra (1, Ti 2p; 2, Mo 3d and 3, S 2p) of MoS₂/TiO₂ microspheres with various morphologies: a, core–shell structure; b) yolk–shell structure; c) hollow structure.

Table S1. BET measurement and the amount of Ti in the resultant samples.

Sample	TiO ₂ -anatase	MoS ₂	TiO ₂ /MoS	y-TiO ₂ /MoS	h-TiO ₂ /MoS
	2	2	2	2	2

S _{BET} (m ² /g)	137	35	287	231	129
TiO ₂ (%)			92.59	81.81	60.61

Table S2. The adsorption value and degradation rate of resultant samples towards MB

Sample	TiO ₂	TiO ₂ -anatase	MoS ₂	TiO ₂ /MoS ₂	y-TiO ₂ /MoS ₂	h-TiO ₂ /MoS ₂
Adsorption value (mg·g ⁻¹)	189.7	130.4	396.6	299.97	498.5	498.5
Degradation rate (%)	27.55	60.1	67.76	84.56	93.39	98.28

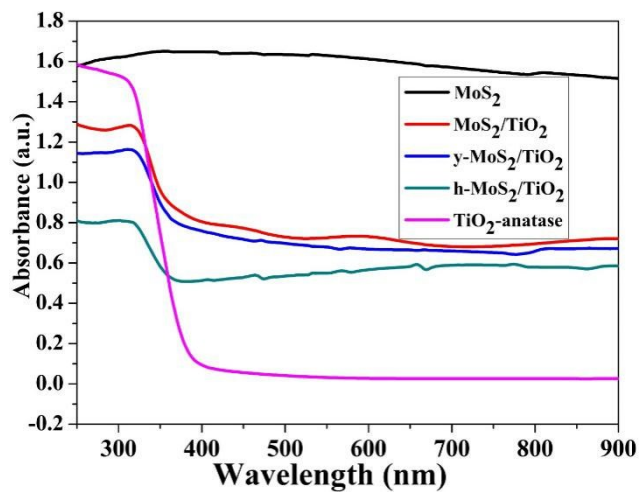


Figure S6. UV–vis absorption spectra of resultant samples.

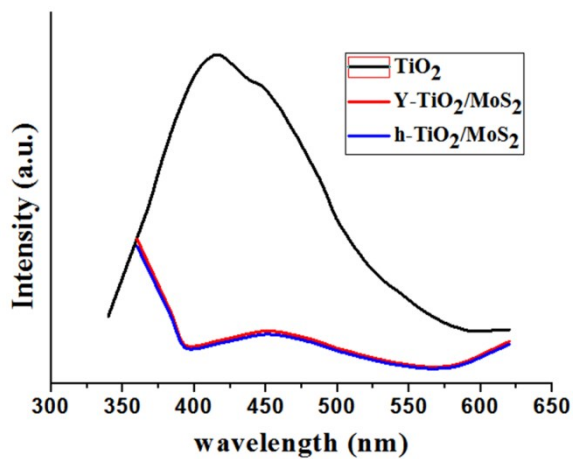


Figure S7. the photoluminescence spectra of TiO₂, h-TiO₂/MoS₂ and y-TiO₂/MoS₂

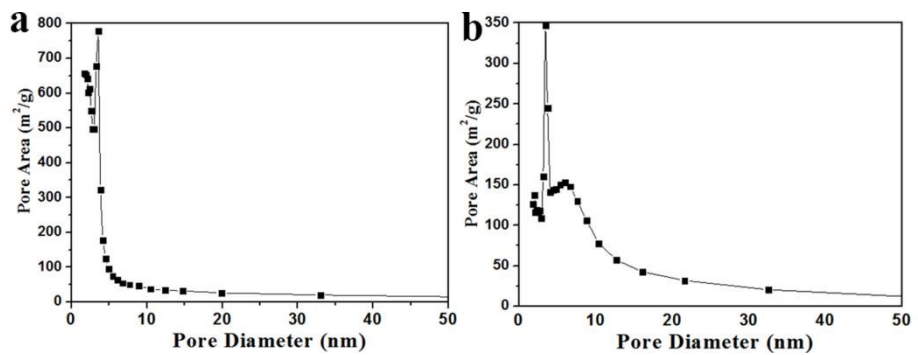


Figure S8. pore-size distribution curves of $\text{MoS}_2/\text{TiO}_2$ heterostructures with various morphologies: a,) yolk–shell structure and b) hollow structure.

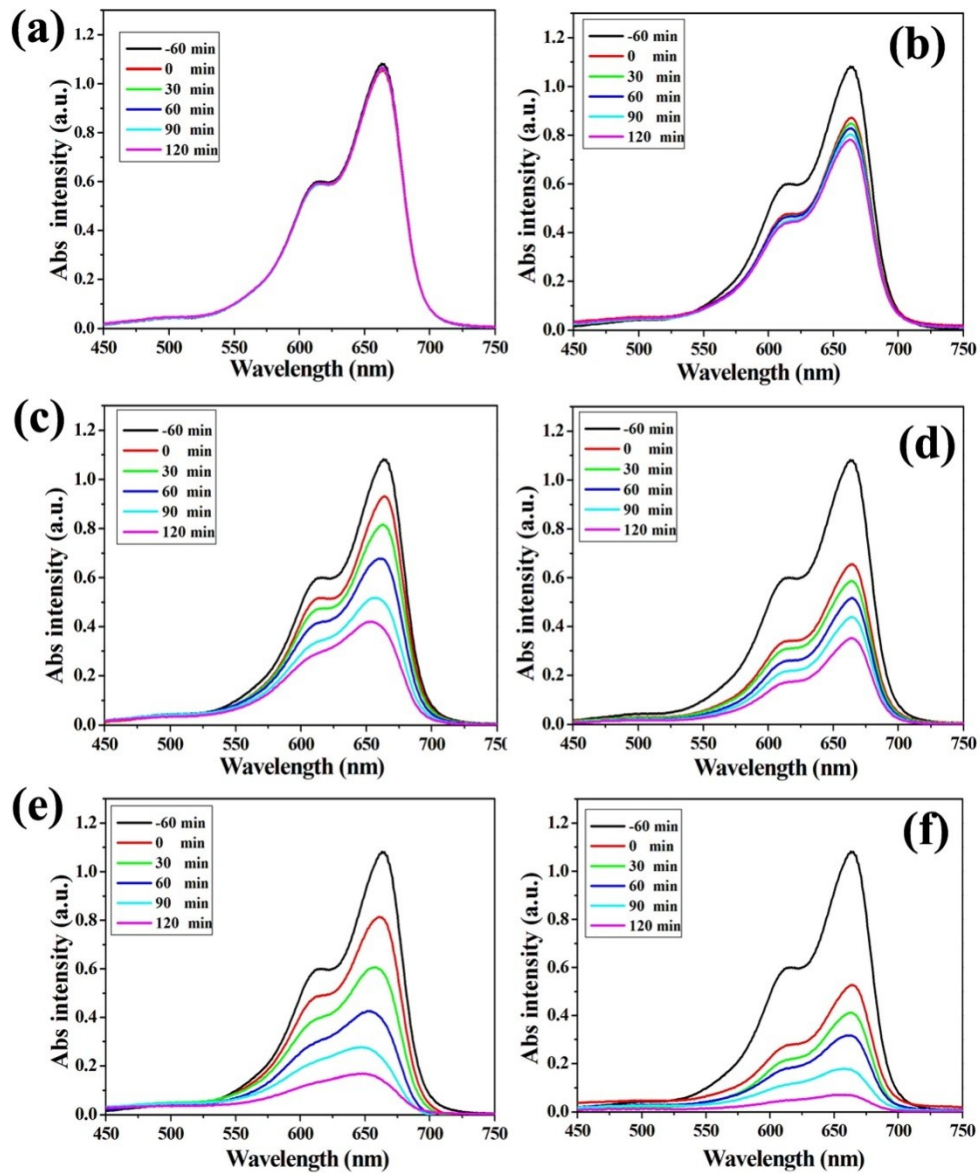


Figure S9. absorption spectra of the solution of MB in the presence of different photocatalysts ($30 \text{ mg}\cdot\text{mL}^{-1}$): a) no catalysts; b) TiO_2 ; c) TiO_2 -anatase; d) pure MoS_2 ; e) $\text{MoS}_2/\text{TiO}_2$ core–shell microspheres; f) $\text{MoS}_2/\text{TiO}_2$ yolk–shell microspheres.

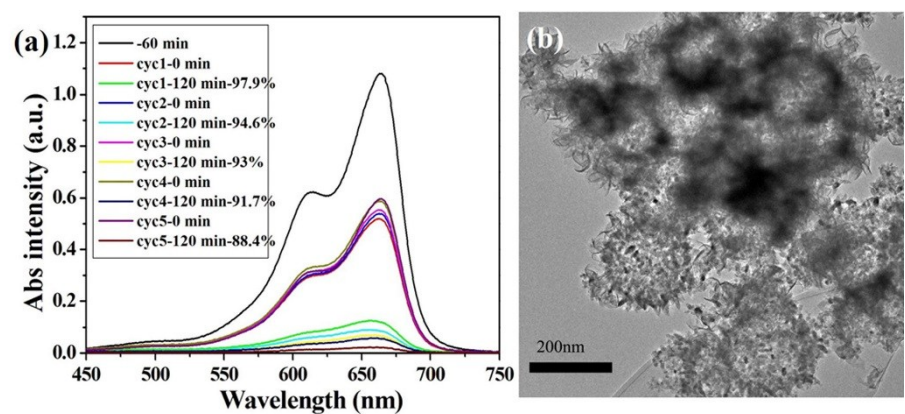


Figure S10 (a) absorption spectra of degradation of MB using $\text{MoS}_2/\text{TiO}_2$ hollow microspheres as the photocatalyst after visible light irradiation for five cycles; (b) TEM image of $\text{MoS}_2/\text{TiO}_2$ hollow microspheres after photocatalytic degradation.

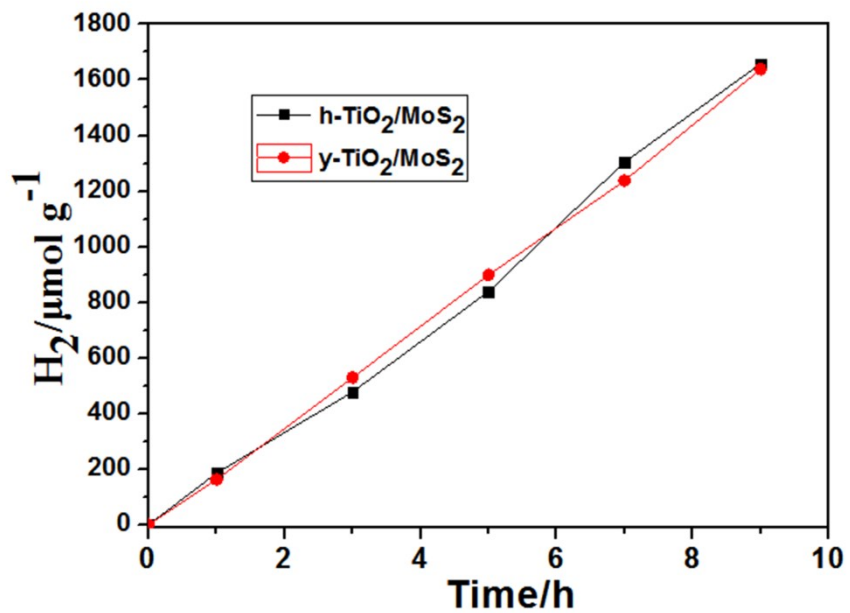


Figure S11. The photocatalytic hydrogen evolution for $\gamma-\text{TiO}_2/\text{MoS}_2$ and $\text{h}-\text{TiO}_2/\text{MoS}_2$